REMOTELY SENSED METHOD FOR DETECTION OF SPATIAL DISTRIBUTION PATTERN OF DRYLAND PLANTS IN WATER LIMITED ECOSYSTEM

Buho Hoshino[1], Ying Tian[1], Keita Shima[1], Su Riga[1], Zoljarga Enkhtuvshin[2], Christopher McCarthy[3], Myagmartseren Purevtseren[4]*

1 Laboratory of Environmental Remote Sensing, Rakuno Gakuen University, Ebetsu, 069-8501, Japan
(* Corresponding author, Buho Hoshino, aosier@rakuno.ac.jp)
2 Mongolian Hydrological, Meteorological and Environmental Center of Sainshand, Mongolia
3 University of California San Diego, 9500 Gilman Dr, La Jolla, CA 92093, USA
4 Department of Geography, National University of Mongolia, Ulaanbaatar 14200, Mongolia

ABSTRACT

The Gobi Desert in Mongolia is characterized by sparse and patchy vegetation, interspersed with essentially bare areas. The vegetation pattern is typically formed by perennial shrubs, grasses or annually-herbaceous plant overlying a matrix composed of bare soil. Vegetation patterns, most broadly, refer to the spatial organization of vegetation in a landscape. However, since the plants in the Gobi Desert are sparsely distributed over a vast bare field, it is extremely difficult to accurately observe from satellite imagery. This is because reflectance of dry soil is very high and the reflectance of slightly distributed plants is eliminated by soil reflection. This study solves this problem by using field surveys and methods for combining different satellite sensor data and spectral un-mixing analysis. As a result, the pixel NDVI value of desert plants shows a smaller value than the ground measurement. It is shown that the fraction of the vegetation endmember after pixel un-mixing has a remarkably high correlation with the field measured values (where, R2=0.51 between NDVI of Landsat 8 imagery original pixels and un-mixed pixels and R2=0.79 between plants coverage of field measurement and un-mixed pixels percentage of vegetation endmembers).

***Index Terms*—**Spectral un-mixing, spatial distribution pattern of dryland plants, Landsat, field measurement.

1. INTRODUCTION

Arid and semi-arid drylands account for 41.3% of the Earth’s surface. Globally, 2.1 billion people live in dryland environments, meaning that drylands are home to one in three people. According to UN-Habitat, the 18.5% population growth rate in drylands was faster than that of any other ecological zone [1-2].

Desertification refers to degradation of land in arid, semi-arid and sub-humid areas resulting from various factors, including climatic variations and human activities. When land degradation occurs in the world's drylands, it often creates desert-like conditions. Globally, 24% of all terrestrial lands is degrading. About 1.5 billion people directly depend on these degraded areas. Nearly 20% of the degrading land is cropland, and 20-25%, rangeland, of which the grasslands of the Mongolian plateau are classified [2-3].

Vegetation patterns have a global distribution in semi-arid ecosystems, suggesting that rather than being a species or area-species trait, the phenomenon of vegetation patterning arises as a response to environmental conditions in these regions [4]. Ecological pattern formation at the level of whole ecosystems is a new, exciting, and rapidly growing research area, whose study is influenced strongly by Turing’s ideas of pattern formation theory. Self-organised patterns of vegetation are a characteristic feature of many semi-arid regions. Mathematical modelling is widely used to study these banded patterns, because there are no laboratory replicates [5]. However, since the plants in the Gobi Desert are sparsely distributed (dot distributed pattern) over a vast bare field, it is extremely difficult to accurately observe from the satellite imagery. Accurately grasping the physiological and ecological characteristics of plants in desert areas and the distribution of plants is very important for preserving endemic species and validation of afforestation efficiency in drylands [4-5].

In this study, we first used Linear Spectral Unmixing (LSU) to determine the relative abundance of vegetation that is depicted in multispectral satellite imagery based on vegetation-bare soil-water spectral characteristics. Second, we setup 20 plots at 4-sites within different rainfall regions and conducted field surveys to measure the coverage, height and spectral reflectance of plants in the Gobi Desert region. We verified the result of spectral un-mixing using field survey data, suggesting that there is a high correlation.

2. MATERIALS AND METHODS

$$\frac{\partial n}{\partial t} = \frac{\gamma\omega}{1+\sigma\omega} n - n^2 - \mu n + \nabla^2 n \quad (1)$$

$$\frac{\partial \omega}{\partial t} = \mathrm{P} - (1-\rho n)\omega - \omega^2 n + \delta\nabla^2(\omega - \beta n) - \nu \frac{\partial(\omega - \alpha n)}{\partial x} \quad (2)$$

2.1 The Study Area

Four sites (size of 250 square meters) with different annual rainfall amounts were selected as study areas, and five plots of 10 square meters were set up in each site (see Fig. 1a). The northern most site, located at Ulaanbaatar, is a semi-arid area, with annual rainfall about 300 mm. The southernmost site, located in the Gobi Desert (Tsogt-Ovoo, site1) is an arid area, where annual rainfall is 40 mm or less. However, annual rainfall during 2007 and 2016 at both of these sites showed an increasing trend. There was no significant change in the annual average temperature.

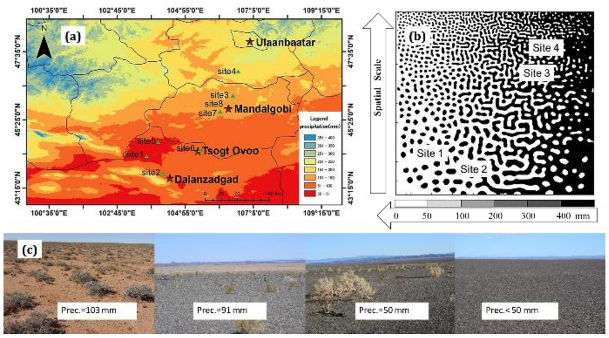

Fig. 1 (a) Map of annual precipitation and location of study sites (UB-Ulaanbaatar City (site 4); MG-Mandal Gobi (site 3); DZ-Dalanzadgad (site 2); and TO-Tsogt-Ovoo (site 1); (b) Distribution pattern of plants in drylands of Mongolia (The horizontal axis shows annual mean precipitation); (c) Field photos at different precipitation points.

2.2 Data analysis

2.2.1 Ground Truth Data

The leaf scale spectral reflectance's (the photosynthetic activity of leaves), plant volume (cm3) and soil moisture in the plot were measured during the spring and summer of 2015-2018.

2.2.2 Calculation of survival ratio of plants

Hardenberg et al. (2004) [6] and Kéfi, et al. (2007) [7-8] developed the vegetation patches formation and spatial vegetation patterns model in "water-limited ecosystems" (see equation (1)(2)). Among these, for the biomass density ***n(x, t)*** and, the logistic equation (1st term-plant growth, where is dry matter productivity (DMP) and fourth item-plant dispersal) which has a positive correlation with moisture in the formula (1), and the amount of the 2nd and 3rd variables shows the vegetation loss due to livestock and wildlife feeding. For the groundwater density ***w(x, t)***, including rainfall **P** (the 1st variable), evaporation (the 2nd variable suppressed by vegetation), and groundwater and soil moisture uptake by plants (3rd variable) and downhill flow (4th variable) according to the equation (2). This research realized the field verification of this equation.

In this study, we calculated how long the vegetation that grew in summer survived through autumn and winter and the following spring. To calculate the survival ratio of plants we used the following equation,

$$Ratio^{NDVI} = \frac{NDVI^{spring}}{NDVI^{previous\ summer}} \quad (3)$$

2.2.3 Linear Spectral Un-mixing

The reflectance at each pixel of the image is assumed to be a linear combination of the reflectance of each material (or endmember) present within the pixel. The fundamental concept underlying Linear Unmixing calculations is that each pixel in the spectral image is categorized as representing a mixture of endmember signals (intensities) when the measured spectrum (M(λ)) can be deconvolved into the proportion (P) of each individual endmember reference spectrum (R(λ)) when the values are summed. Thus, each reference spectrum of a pure endmember is described as Ri(λ) where i = 1,2,3.....N represents the index of the end members (Pi). For a particular number of endmembers (n), this relationship can be represented as [9]:

$$M(\lambda) = \sum_{i=1}^{N} (Pi.Ri(\lambda)) \quad (4)$$

Where **M (λ)** is the effective reflectance of the mixed pixel; **Pi** is the spatial fraction covered by the ith material; **Ri(λ)** is the reflectance of the ith endmember; **N** is the number of materials in the pixel; **λ** is a band (or wavelength).

Given the resulting spectrum (the input data) and the endmember spectra, Linear Spectral Unmixing solves for the abundance values of each endmember for every pixel. The number of endmembers must be less than the number of spectral bands, and all of the endmembers in the image must be used. Spectral unmixing results are highly dependent on the input endmembers; changing the endmembers changes the results. For many Linear Unmixing software packages, the solution is obtained by inputting reference spectral profiles and using an inverse least squares fitting approach that minimizes the square difference between the measured and the calculated spectra.

Linear Spectral Unmixing has two constraint options: unconstrained or a partially constrained unmixing. In the unconstrained method, abundances may assume negative values and are not constrained to sum-to-unity. In this study, we use ENVI software methodology. The ENVI methods also support an optional, variable-weight, unit-sum constraint in the linear-mixing algorithm. This allows you to define the weight of a sum-to-unity constraint on the abundance fractions. It also permits proper unmixing of MNF transform data, with zero-mean bands.

3 RESULTS

3.1 Calculation and measurement results of plant survival rate

As shown in Fig. 2, the ratio of NDVI calculated from the Landsat 8 satellite data (equation (3)) was very low in the annual plants distribution area and very high in the perennial plants distribution area. It has been shown that perennial shrubs, such as Saxaul tree (*Haloxylon ammodendron*) can survive the extremely dry environment and winter season in the Gobi Desert region harsh condition of Mongolia.

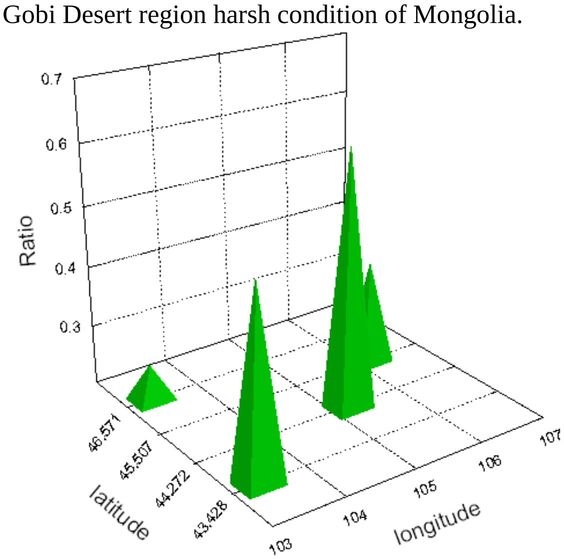

Fig. 2 The survival ratio NDVI calculation results for perennial and annual plants (where, the upper part of the image shows the annual plant area, and the lower part of image shows the perennial plant area).

A high NDVI ratio indicates a high plant survival rate. Plant loss is primarily due to feeding by livestock and wildlife, loss of moisture, and movement by wind. The remaining plants can be used as livestock feed, and can suppress desert and dust storms. As shown in Fig. 2, it was suggested that the residual quantity of annual plants at the Ulaanbaatar study site is small, and the residual quantity is higher at the Gobi Desert sites (TO, DZ) where perennial plants are dominant. Fig. 3 shows field measurements of plants coverage at the study sites.

The result was opposite to the survival rate of plants (or NDVI ratio). In other words, it showed a high value in the annual plants distribution area and a low value in the perennial distribution area.

3.2 Vegetation pattern and the spatial fractional coverage of Gobi plants

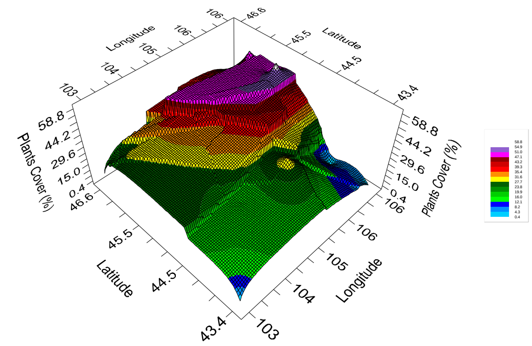

Fig. 3 Field measurement of average value of plant coverage (%) in (10m ×10m) quadrat area

In semi-arid areas where annual precipitation is more than 150 mm, annual herbaceous plants are dense, so the landscape is like a green carpet. However, in arid areas where annual precipitation is 150 mm or less, the perennial shrubs are sparsely distributed in dotted patterns across bare land (see Fig. 4).

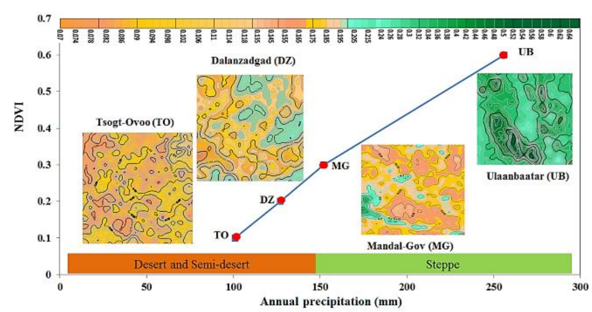

Fig. 4 Simulation results of dimensionless biomass (NDVI) along a gradient of decreasing water stress (precipitation) for (UB) – Ulaanbaatar; (MG)-Mandal-Gov; (DZ)-Dalanzadgad; and (TO)-Tsogt-Ovoo based on simplified equation (1) and (2). To refine the representation of biomass transport, the diffusion term in the P equation is replaced by a convolution of a dispersion kernel and standing biomass, defining the seed rain about a parent plant.

In the Gobi Desert region, plants are sparsely distributed across bare ground. In such places, it is difficult to estimate accurate plant quantity from intermediate resolution satellite data like Landsat imagery. In this paper, the linear unmixing method (equation (4)) is used to decompose pixels of Landsat 8 satellite imagery and the results were verified in the field. Comparing the NDVI calculated from the calibrated pixels (reflectance of pixels) of the Landsat 8 satellite data in the target pixel shown in Fig. 5(a,b). It was suggested that there is a high correlation between the NDVI original pixels and the unmixing pixels in Landsat 8 imagery.

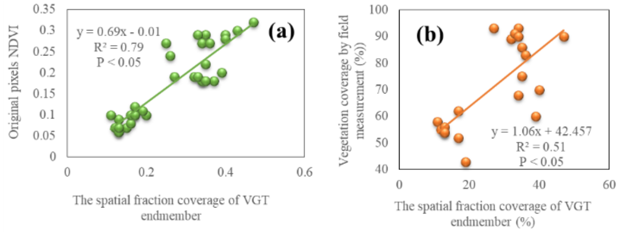

Fig. 5 Comparision result of the NDVI value of Landsat 8 original pixels (left panel) and the field measurement of vegetation coverage (%) with the Landsat 8 pixels unmixing spatial fraction coverage of vegetation (VGT) in the same target pixel of each plot.

Comparing the Landsat 8 pixels unmixing spatial fraction coverage of vegetation (VGT) with field measurements of vegetation coverage in the target pixel of each plot, it was suggested that there is a high correlation between the unmixing pixels in Landsat 8 imagery and field measurement of vegetation coverage. The spatial resolution of Landsat satellite data was 30 square meters, while the size of the plant identification survey in the field was 10 square meters. As a result, the variability increased in semi-arid areas where the percentage of vegetation covered by annual herbaceous plants was 40%. The measured value and the unmixing fraction coverage value showed a very high correlation at the site where the vegetation coverage was 50% or 10%.

4 DISCUSSION

Pattern-formation theory predicts that vegetation gap patterns, such as those found in the harsh condition of Mongolia's Gobi Desert region, emerge through the action of pattern-forming biomass–water feedbacks and that such patterns should be found elsewhere in water-limited systems around the world [5]. We report here the exciting discovery of self-organized patterns (dot distribution patterns) of vegetation in the Gobi Desert of Mongolia. Using fieldwork, remote sensing, spatial pattern analysis, mathematical modeling, and pattern-formation theory we show that self-organized patterns do in fact occur in the Gobi Desert of Mongolia. Since the plants in the Gobi Desert are dot distributed over bare ground, the satellite pixel synthesized there is greatly influenced by the high reflection of background bare soil [10-12]. In areas where annually low grass vegetation is sparsely distributed, even when the vegetation coverage is 40%, the values when synthesizing the satellite pixels vary greatly between the measured values. As a result, the variability increased in semi-arid areas where the percentage of vegetation covered by annual herbaceous plants was 40%. The measured value and the unmixing fraction coverage value showed a very high correlation at the study site where the vegetation coverage was 50% or 10%. Where, the areas with 10% vegetation coverage are Gobi Desert sites and the site with 40% vegetation coverage is degraded pasture land near the capital city of Ulaanbaatar.

5. ACKNOWLEDGMENT

This work was supported by JSPS KAKENHI Grant Numbers: JP18H03608 and JP19H04362.

6. REFERENCES

[1] Millennium Ecosystem Assessment: "*Ecosystems and Human Well-being: Synthesis".* Island Press, Washington, DC. 2005.

[2] GEF-STAP, "Report of the Scientific and Technical Advisory Panel to the Fourth GEF Assembly". 2010.

[3] Sofue, Y., Hoshino, B., Demura, Y., Nduati, E., and Kondoh, A., "The Interactions Between Precipitation, Vegetation and Dust Emission Over Semi-Arid Mongolia", Atmos. Chem. Phys. Discuss., doi:10.5194/acp-2017-83, in review, 2017.

[4] V. Deblauwe, N. Barbier, P. Couteron, O. Lejeune, and J. Bogaert. The global biogeography of semi-arid periodic vegetation patterns. Global Ecology and Biogeography, 17(6):715-723, 2008.

[5] G. Stephan, Y. Hezi, B. Bronwyn et al.. Discovery of fairy circles in Australia supports self-organization theory. PNSA, 2016. doi: 10.1073/pnas.1522130113.

[6] von Hardenburg, J. and Meron, E. and Shachak, Moshe and Zarmi, Y. "Diversity of vegetation patterns and desertification". *Physical Review Letters*, 87(19), 2001.

[7] Kéfi, Sonia, Rietkerk, Max, Alados, et al., "Spatial vegetation patterns and imminent desertification in Mediterranean arid ecosystems", *Nature*, 449, 213-7. 2007.

[8] Max Rietkerk, Stefan C. Dekker, Peter C. de Ruiter, Johan van de Koppel. "Self-Organized Patchiness and Catastrophic Shifts in Ecosystems", *Science* 305 (5692), 1926-1929. 2004.

[9] Garini, Y.; Young, I.T.; McNamara, G. "Spectral imaging: Principles and Applications". Cytometry Part A. 69, 735–747. 2006.

[10] Buhe Aosier, Tsuchiya, K. Kaneko, M. Ohtaishi, N. Halik, Mahmut. "Land cover of oases and forest in XinJiang, China retrieved from ASTER data", *Advances in Space Research* 39(1), 39-45, 2007.

[11] Hoshino B, Yonemori M, Manayeva K, Karamalla A, Yoda k, Suliman M, Elgamri M, Nawata H, Mori Y, Yabuki S. "In Remote Sensing Methods for the evaluation of the mesquite tree (prosopis juliflora) environmental adaptation to semi-arid Africa", IEEE International Geoscience and Remote Sensing Symposium (IGARSS), 1910-1913. 2011.

[12] Na YT, Bao S, Hashimo K, Mccarthy C, Hoshino B. "The Effects of Grazing Systems on Plant Communities in Steppe lands—A Case Study from Mongolian's Pastoralists and Inner Mongolian Settlement Areas". Land, vol. 7,1-10. 2018.